

Out-of-equilibrium dynamics of multiple second-order quantum phase transitions in extended Bose-Hubbard model: Superfluid, supersolid and density wave

Keita Shimizu¹, Takahiro Hirano¹, Jonghoon Park¹, Yoshihito Kuno², and Ikuo Ichinose¹

¹*Department of Applied Physics, Nagoya Institute of Technology, Nagoya, 466-8555, Japan* and

²*Department of Physics, Graduate School of Science, Kyoto University, Kyoto, 606-8502, Japan*

(Dated: November 15, 2018)

This paper studies the dynamics of the Bose-Hubbard model with the nearest-neighbor repulsion by using time-dependent Gutzwiller methods. Near the unit fillings, the phase diagram of the model contains density wave (DW), supersolid (SS) and superfluid (SF). The above three phases are separated by two second-order phase transitions. We study “slow-quench” dynamics by varying the hopping parameters in the Hamiltonian as a function of time. In the phase transition from the DW to SS and SF, we focus on how the SF order forms and study scaling laws of the SF correlation length, vortex density, etc. The results are compared with the Kibble-Zureck scaling. On the other hand from the SF to DW, we study how the DW order evolves and generation of the domain walls and vortices. Measurement of first-order SF coherence reveals interesting behavior in the DW regime.

PACS numbers: 67.85.Hj, 03.75.Kk, 05.30.Rt

I. INTRODUCTION

Systems of ultra-cold atomic gases have the high versatility and controllability. In the last decades, ultra-cold atomic gas systems play an important role for the study on the quantum many physics as quantum simulators [1–4]. In this paper, we study ultra-cold Bose gas systems as a quantum simulator for out-of-equilibrium dynamics of many-body quantum systems. For a finite-temperature quench, from the view point of the cosmology, Kibble [5, 6] studied how the system exhibits out-of-equilibrium behavior and pointed out that the phase transitions lead to topological defects as a result of spontaneous symmetry breaking of continuous symmetries. After the pioneering work by Kibble, Zurek [7–9] found that a similar phenomenon is to be observed in experiments on the condensed matter systems such as the superfluid (SF) of ^4He . Furthermore for the second-order phase transition, it was argued that physical quantities satisfy some kind of scaling laws with respect to the quench time that measures the speed of the “slow quench”. The works by Kibble and Zurek stimulated many physicists, and there appeared many theoretical and experimental studies to test this conjecture, which is sometimes called Kibble-Zureck (KZ) mechanism and KZ scaling [10]. Recent experiments on ultra-cold atomic gases in a homogeneous density setup verified the KZ scaling law for the correlation length and topological defect formation [11, 12].

Similar problem was also studied for quantum systems, i.e., how low-energy states evolve under a change of the parameters in the Hamiltonian crossing a quantum phase transition (QPT), i.e., the quantum quench [13–19]. This problem has also attracted great interest. Experiments on behaviors of quantum systems through QPTs were already done using the ultra-cold atomic gases as a quantum simulator [20–24].

In the previous two papers [25, 26], we study the out-of-equilibrium dynamics of the ultra-cold Bose atoms on

a square optical lattice by using the Bose-Hubbard models. In the practical calculation, we fixed the on-site and nearest-neighbor (NN) repulsions and varied the hopping amplitude in the Hamiltonian, and studied how the lowest-energy state evolves. In Ref [25], we investigated how the ground state evolves from the Mott insulator to SF by means of the time-dependent Gutzwiller (GW) methods. We first showed the behavior of the SF order parameter, and gave physical pictures of the out-of-equilibrium behavior of the system. We found that the physical quantities such as the correlation length of the SF, vortex density, etc. satisfy scaling laws and compared the obtained scaling exponents with the predicted values given in terms of the critical exponents of the static phase transition via the KZ hypothesis. On the other hand in Ref. [26], we considered extended Bose-Hubbard model, which includes the NN repulsion. Phase diagram has the SF, density wave (DW) and also the supersolid (SS). For fairly weak NN repulsion, there exists a first-order phase transition directly connecting the DW and SF phases accompanying a finite jump in physical quantities [27, 28]. We focused on that parameter regime, and studied the quench dynamics from the DW to SF, and vice-versa.

In this work, we consider the intermediate strength of the NN repulsion. As a result, there exist two second-order phase transitions separating the DW and SS, and also the SS and SF [27, 28]. Therefore, dynamics of an out-of-equilibrium multiple phase transition can be discussed.

This paper is organized as follows. In Sec. II, we introduce the extended Bose-Hubbard model on the square lattice, and define order parameters used to distinguish various phases. Equilibrium phase diagram obtained by the static GW methods is shown. There are three phases, i.e., DW, SS and SF.

In Sec. III, we show the results of the quench dynamics from the DW to SS, and also from the DW to SF through the SS. Behavior of the SF order parameter is

investigated in detail and see if scaling laws of the SF correlation length, etc, hold. The results are compared with the KZ mechanism, and estimation of the critical exponents is given. We also calculate the SF correlation length in the SF regime and examine what kind of state forms there.

In Sec. IV, we study quench dynamics from the SF to DW through SS. Behavior of the SF order parameter depends on the quench time τ_Q . For small τ_Q (fast quench), domain walls of finite-size DWs form and the amplitude of the SF remains finite. We also show that quantum vortices are bound on domain walls. On the other hand for large τ_Q (slow quench), individual DW region is large. However, the first-order correlation of the boson operator has a peculiar behavior. Its origin is discussed.

Section V is devoted for conclusion and discussion.

II. EXTENDED BOSE-HUBBARD MODEL AND EQUILIBRIUM PHASE DIAGRAM

We consider the two-dimensional extended Bose-Hubbard model (EBHM) described by the following Hamiltonian,

$$H_{\text{EBH}} = -J \sum_{\langle i,j \rangle} (a_i^\dagger a_j + \text{H.c.}) + \frac{U}{2} \sum_i n_i(n_i - 1) + V \sum_{\langle i,j \rangle} n_i n_j - \mu \sum_i n_i, \quad (1)$$

where $\langle i,j \rangle$ denotes a pair of NN sites of a square lattice, a_i^\dagger (a_i) is the creation (annihilation) operator of boson at site i , and $n_i = a_i^\dagger a_i$. J is the hopping amplitude, and μ is the chemical potential. There are two kind of repulsions in the model, i.e., U and V -terms in Eq.(1), which describe the on-site and NN repulsions, respectively. For $J, V < U$, the system is in the Mott insulator, whereas for $J > U, V$, the SF forms. On the other hand for $V > J, U$, the DW order is realized. As we see later on, there exists another phase, i.e., SS, which has both the DW and SF orders.

In this paper, we consider the system near the unit filling $\rho = \frac{1}{N_s} \sum_i \langle n_i \rangle = 1$, where N_s is the number of lattice sites. In most of the practical calculations, we set $N_s = 64 \times 64$ with the periodic boundary condition. In the previous work [26], we focused on the system near the half filling $\rho = 1/2$ and weak NN repulsion such as $V/U = 0.05$, and studied the first-order phase transition between the DW and SF. On the other hand in this work, we consider the case $\rho \approx 1$ and relatively large V , and study the phase transitions including the DW, SS and SF.

In order to obtain the phase diagram, we calculate the following order parameters to distinguish the above men-

tioned states,

$$\begin{aligned} \Psi_i &= \langle a_i \rangle, \quad |\Psi| = \frac{1}{N_s} \sum_i |\Psi_i|, \\ \Delta_{\text{DW}} &= \frac{1}{N_s} \sum_i (-1)^i \langle n_i \rangle, \\ \Delta_{\text{SF}} &= \frac{1}{N_s} \sum_i (-1)^i |\Psi_i|, \end{aligned} \quad (2)$$

where $(-1)^i$ stands for $+1$ (-1) for even sites (odd sites). In Eq.(2), Ψ_i and $|\Psi|$ measure the SF order, and Δ_{DW} for the DW, whereas a finite Δ_{SF} indicates the existence of the SS, which is called relative order parameter [29]. In the study of the non-equilibrium quench dynamics, the above quantities play an important role and they are measured as a function of time.

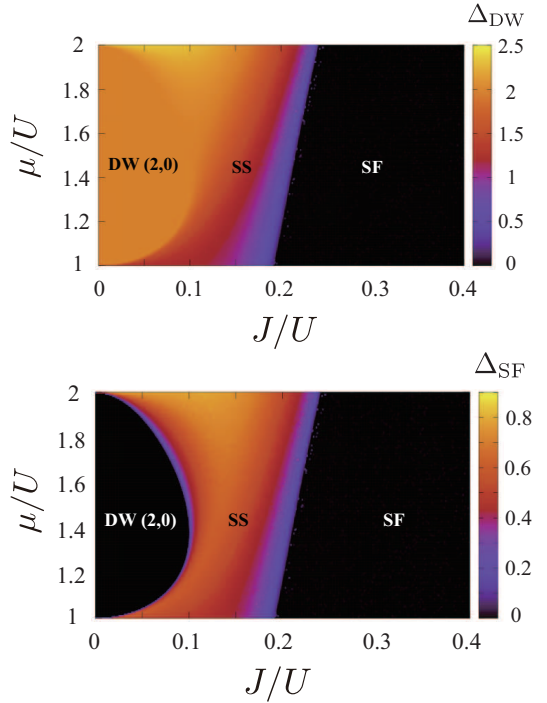


FIG. 1. Phase diagrams of the EBHM near the unit filling and $V/U = 0.375$. There are three phases, (2,0)-type DW, SS and SF. These phases are separated by the second-order phase transitions.

Before going into the out-of-equilibrium dynamics of the system, we show the equilibrium phase diagram of the EBHM for $V/U = 0.375$ in Fig. 1 and the physical quantities in Fig. 2, which are calculated by the static GW methods and used for identification of phases. There are three phases for $V/U = 0.375$, i.e., the SF, DW and SS. The SS has both the SF and DW order, and is located between the SF and DW in the phase diagram. There are two phase boundaries, and both phase transitions are of second order as the physical quantities in Fig. 2 indicate. This result is in good agreement with that of

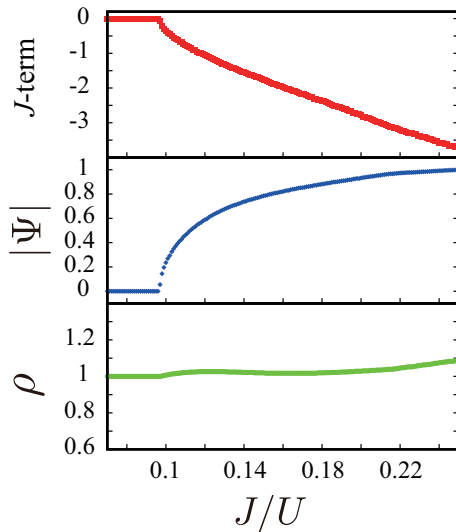


FIG. 2. Calculations of the physical quantities for the phase diagrams in Fig. 1. Chemical potential $\mu/U = 1.5$ and $V/U = 0.375$. J -term stands for the expectation value of the hopping term $-\sum_{\langle i,j \rangle} (a_i^\dagger a_j + \text{H.c.})$.

the previous study using quantum Monte-Carlo (QMC) simulations [28] although the regions of the SS phases are slightly larger than the QMC results.

In the subsequent sections, based on the phase diagram in Fig. 1, we shall study out-of-equilibrium quench dynamics of the system that takes place when the system is crossing the phase boundaries as a result of temporal change in parameters in the Hamiltonian in Eq.(1). In the practical calculation, we fix $U = 1$ as the unit of energy, and also we focus on the case with $V = 0.375$ as in the static case. In the previous work [26], we studied the system with $V = 0.05$, in which the SS does not form near $\rho \approx 0.5$ and a first-order phase boundary exists between the SF and DW. In the present work, we are interested in how the system evolves when it crosses the multiple second-order phase transitions, etc.

III. TRANSITION FROM DW TO SS AND SF

In this section, we consider the dynamics of the transitions from the DW to SS and SF. As shown in Fig. 3, the mean particle density $\rho \approx 1$ for $\mu/U = 1.5$, and then the DW is the (2,0)-type one. Phase transition from the DW to SS takes place at $J = J_{c1} \simeq 0.10$, and from the SS to SF at $J = J_{c2} \simeq 0.22$, respectively.

We consider the transition from the DW to SS first, and employ the time-dependent GW (tGW) methods to study the out-of-equilibrium dynamics. In the practical calculation, the following quench protocol is used;

$$\frac{J(t) - J_{c1}}{J_{c1}} = \frac{t}{\tau_Q}, \quad t \in [-\tau_Q, \tau_Q], \quad (3)$$

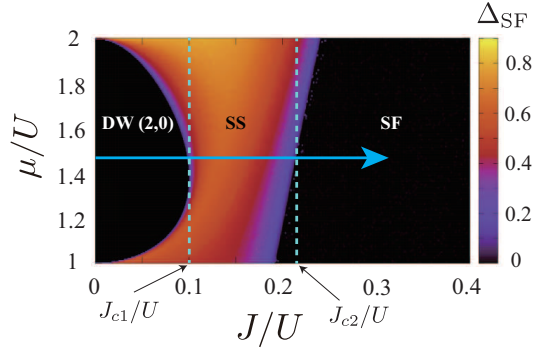


FIG. 3. Quench protocol from the DW to SS and SF in the phase diagram in Fig. 1. For $\mu/U = 1.5$, the critical points are located at $J_{c1}/U = 0.10$ and $J_{c2}/U = 0.22$.

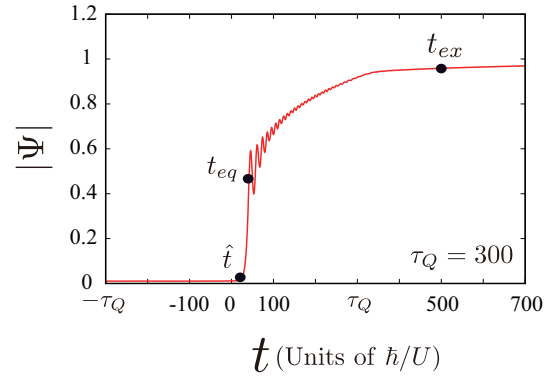


FIG. 4. SF amplitude from the DW to SS as a function of time. At $t = 0$, the system passes through the equilibrium phase transition point DW \rightarrow SS. Locations of \hat{t} , t_{eq} and t_{ex} are indicated.

where τ_Q is called quench time. The protocol in Eq.(3) indicates that the system crosses the equilibrium phase transition point J_{c1} at $t = 0$, and the quench terminates at $t = \tau_Q$ with $J(\tau_Q) = 2J_{c1} (< J_{c2})$.

In Fig. 4, we show the SF order parameter $|\Psi|$ as a function of time (t) for $\tau_Q = 300$. Ψ exhibits a similar behavior to that in the transition from the Mott to SF in the $V = 0$ case studied previously. As in the previous works, we define the transition time \hat{t} from the frozen to adiabatic regimes by $\Psi(\hat{t}) = 2\Psi(0)$ [25]. On the other hand, t_{eq} is the time at which the oscillating behavior of Ψ starts. Physical picture of the oscillating regime was explained in the previous paper [25]. The amplitude of SF, Ψ , develops quite rapidly from \hat{t} to t_{eq} . On the other hand, the correlation length only doubles in that period. Genuine coarsening process of the long-range SF coherence takes place between t_{eq} to t_{ex} , where t_{ex} is the time at which the oscillation of Ψ terminates.

It is quite interesting and important to see if scaling laws of physical quantities, such as the SF correlation length and vortex density, with respect to the quench

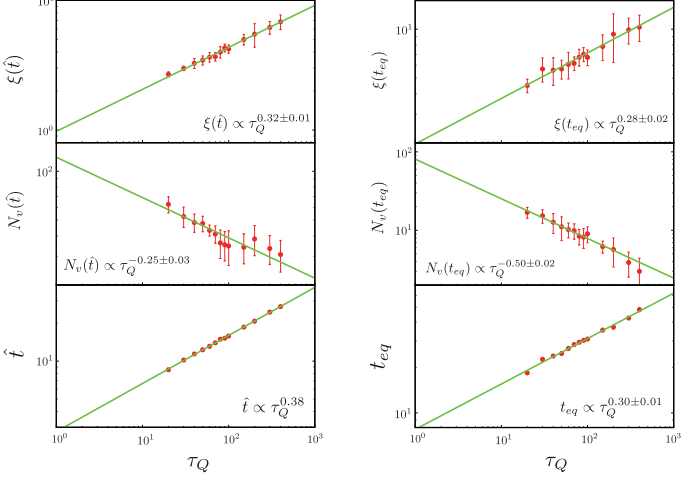


FIG. 5. Observation of scaling laws with respect to τ_Q for various quantities at $t = \hat{t}$ and $t = t_{\text{eq}}$.

time τ_Q hold or not. Here, the SF correlation length and vortex density are defined as

$$\langle a_i^\dagger a_j \rangle \propto \exp(-|i - j|/\xi),$$

$$N_v = \sum_i |\Omega_i|,$$

$$\Omega_i = \frac{1}{4} \left[\sin(\theta_{i+\hat{x}} - \theta_i) + \sin(\theta_{i+\hat{x}+\hat{y}} - \theta_{i+\hat{x}}) - \sin(\theta_{i+\hat{x}+\hat{y}} - \theta_{i+\hat{y}}) - \sin(\theta_{i+\hat{y}} - \theta_i) \right], \quad (4)$$

where θ_i is the phase of Ψ_i and \hat{x} (\hat{y}) is the unit vector in the x (y) direction. As the transition from the DW to SS is a second-order phase transition, one may expect that the correlation length, ξ , and the vortex density, N_v , satisfy a scaling law with the critical exponents of the 3D XY model. However, the DW and (critical regime of) SS are not homogeneous and also there exists the NN repulsions, and then a simple relation between the exponents such as $d = 2b$ may not hold, where exponent b for $\xi \propto \tau_Q^b$, and d for $N_v \propto \tau_Q^{-d}$.

We show the obtained results in Fig. 5 for both $t = \hat{t}$ and $t = t_{\text{eq}}$ cases. It is obvious that ξ and N_v both satisfy a fairly good scaling law from $\tau_Q = 20$ to $\tau_Q = 400$. Exponents are estimated as $b = 0.32$ and $d = 0.25$ for $t = \hat{t}$, and $b = 0.28$ and $d = 0.50$ for $t = t_{\text{eq}}$, respectively. The vortex density at $t = t_{\text{eq}}$ is smaller compared to that at $t = \hat{t}$. Then, the interactions between vortices are less effective at $t = t_{\text{eq}}$, and as a result, the expected relation $d \approx 2b$ holds for $t = t_{\text{eq}}$.

We also show the scaling of \hat{t} and t_{eq} with respect to τ_Q in Fig. 5. For a second-order phase transition with the correlation-length exponent ν and dynamical exponent z , the KZ hypothesis gives $\hat{t}, t_{\text{eq}} \propto \tau_Q^{\nu z/1+\nu z}$, $\xi \propto \tau_Q^{\nu/1+\nu z}$ and $N_v \propto \tau_Q^{-2\nu/1+\nu z}$. From the above results, we can estimate the critical exponents ν and z as $\nu = 0.51$, $z =$

1.18 from the data at \hat{t} , and $\nu = 0.40$, $z = 1.07$ from the data at t_{eq} , respectively. These values are fairly close to those obtained by the mean-field approximation to the 3D XY model, i.e., $\nu = 1/2$ and $z = 1$.

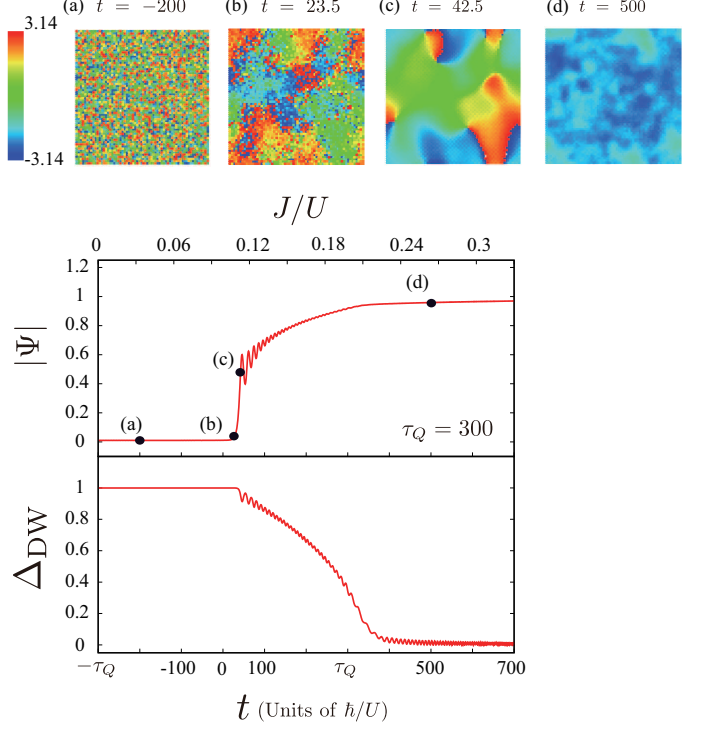


FIG. 6. Slow quench from the DW to SF through the SS. Physical quantities as a function of time for $\tau_Q = 300$. The upper panels show phase of Ψ_i for various times. The system pass through $J = J_{c1}$ (J_{c2}) at $t = 0$ ($t = 1.2\tau_Q$).

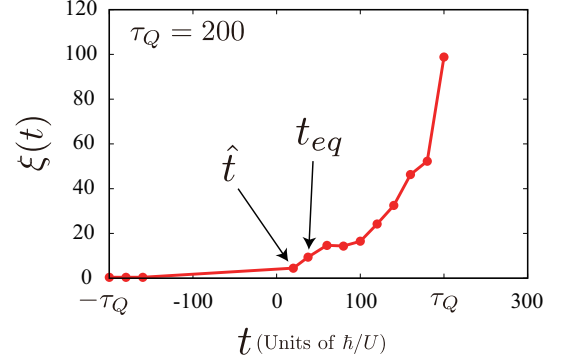


FIG. 7. SF correlation length as a function of time. $\tau_Q = 200$. After t_{eq} , $\xi(t)$ increases quite rapidly. This result indicates that a SF at finite temperature forms there.

Let us turn to the case from the DW to SF through the SS. Quench protocol is as follows,

$$\frac{J(t) - J_{c1}}{J_{c1}} = \frac{t}{\tau_Q}, \quad t \in [-\tau_Q, t_f], \quad (5)$$

where we take the quench-termination time $t_f = 700$ for the case of $\tau_Q = 300$. In Fig. 6, we show the behaviors of Ψ and Δ_{DW} as a function of time for $\tau_Q = 300$. We also show snapshots of the phase of Ψ_i in Fig. 6 (the upper panels). The DW order parameter decreases smoothly after the system passes the point $J/U \approx 0.1$, whereas the SF order parameter increases very rapidly after \hat{t} , and the coarsening process of the phase of Ψ_i takes place smoothly from t_{eq} to t_{ex} . It is interesting to see how the correlation length evolves under the quench, in particular, after the second critical point J_{c2} . The result is shown in Fig. 7. From \hat{t} to t_{eq} , the correlation length doubles, whereas it increases rapidly after t_{eq} as a result of the coarsening process of the phase degrees of freedom of Ψ_i . The calculation in Fig. 7 suggests that the correlation length diverges for large t . This result indicates that SF state *at a finite temperature* forms in that regime and it has a divergent Kosterlitz-Thouless type correlation length, i.e., the quench of the hopping amplitude injects energy into the system, and an equilibrium finite-temperature SF state is realized as a result.

IV. TRANSITION FROM SF TO DW

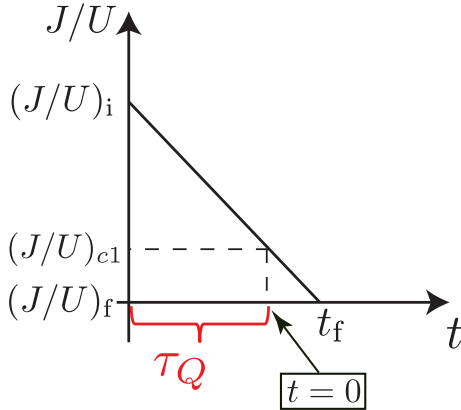


FIG. 8. Quench protocol of out-of equilibrium dynamics in the process SF \rightarrow SS \rightarrow DW.

In this section, we shall study dynamical behavior of the EBHM under the quench from the SF to DW. In the previous paper, we studied a related problem concerning to the first-order phase transition from the SF to the DW. In this work, we consider the case of the multiple-second-order phase transition, i.e., SF \rightarrow SS \rightarrow DW. The practical protocol is the following;

$$\frac{J_{c1} - J(t)}{J_{c1}} = \frac{J_i - J_{c1}}{J_{c1}} \frac{t}{\tau_Q}, \quad t \in [-\tau_Q, t_f], \quad (6)$$

where $J_i = J(-\tau_Q)$ is the initial value of $J(t)$, and we choose as $J_i/U = 0.3 (> J_{c2}/U)$. At $t = 0$, $J(0) = J_{c1}$ and also we choose the final value as $J_f = J(t_f) = 0$, i.e., the quench terminates at $t = t_f = \frac{J_{c1}}{J_i - J_{c1}} \tau_Q$. See Fig. 8.

As the initial state, we use a GW-type wave function, in which small local fluctuations of the phase of $\{\Psi_i\}$ are added to the equilibrium GW ground state. If we start the time evolution with the genuine SF state with a totally coherent phase, a DW-SF heterogeneous state forms as we showed in the previous work for the first-order phase transition.

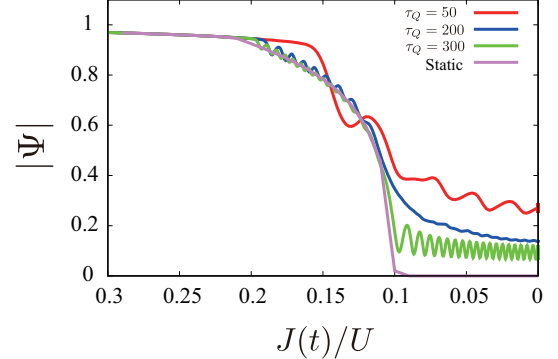


FIG. 9. SF amplitude as a function of J/U for various quench times, τ_Q 's. Results are compared with the equilibrium values.

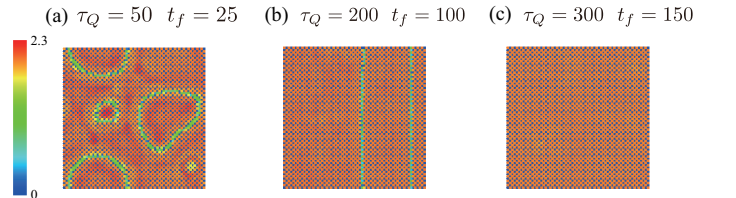


FIG. 10. Density profiles at $t = t_f$ for various quench times, τ_Q 's. $J(t_f) = 0$.

We first show the SF amplitude Ψ as a function of $J(t)/U$ in Fig. 9 for various quench times τ_Q 's. As explained above, $J_{c1}/U \simeq 0.10$ and $J_{c2}/U \simeq 0.22$. For larger τ_Q , the results are getting closer to the static case as it is expected. However in all cases, the SF amplitude $|\Psi|$ has a finite value for $t \rightarrow t_f$.

It is also interesting to see density profile at $t = t_f$ for the above various τ_Q 's. We show the obtained results in Fig. 10. For every τ_Q , there are domain walls separating DW regions, and for larger τ_Q , the less domain walls form. Close look at domain walls shows that the pattern of the DWs changes at domain walls and in domain walls, the expectation value of particle number at each site fluctuates and takes a fractional value.

Next, physical quantities Ψ , Δ_{DW} and Δ_{SF} are shown in Fig. 11 as a function of time for $\tau_Q = 300$. Ψ , Δ_{DW} and Δ_{SF} exhibit expected behaviors. In order to investigate a SF phase coherence in detail, we calculated the first-order

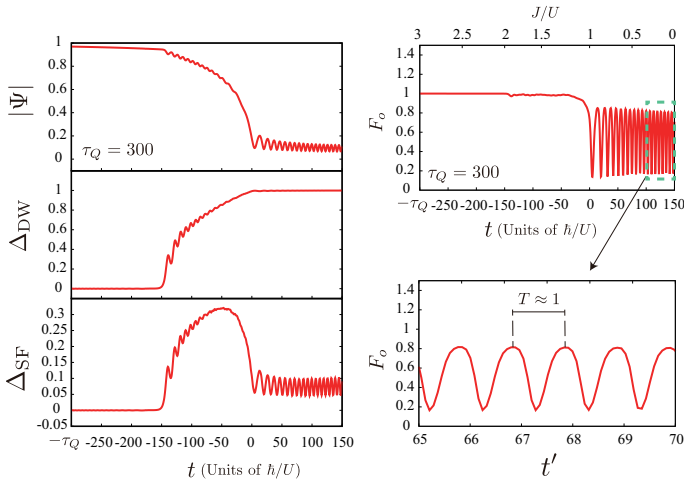


FIG. 11. Left panels: Physical quantities Ψ , Δ_{DW} and Δ_{SF} as a function of time for $\tau_Q = 300$. Right panels: First-order correlation F_o . After $t = 0$, it exhibits the collapse-revival behavior. $t' \equiv t \cdot \frac{U}{2\pi}$. $J(0)/U = J_{c1}/U$ and $J(-150)/U \approx J_{c2}/U$.

correlation defined by

$$F_o = \frac{1}{2N_s} \sum_{i,j} (\langle a_i^\dagger a_j \rangle + \text{c.c.}) \quad (7)$$

In Fig. 11, we show the calculation of F_o for $\tau_Q = 300$ as a function of time. After $t = 0$, F_o exhibits fluctuating behavior and close look at the oscillating regime shows that the period $T \approx 1$. In Fig. 12, we show F_o as a function of time for $\tau_Q = 50, 200$ and 300 . For ever quench time τ_Q , F_o exhibits oscillating behavior after passing $t \approx 0$, but the pattern of oscillation strongly depends on τ_Q . This behavior may be related to the collapse-revival phenomenon that results from the surviving *phase coherence of the SF* as studied in Refs. [30–35]. In fact for the product of the genuine coherent state, $|\text{SF}\rangle = \prod_i |\rho_i, \theta_i\rangle$ with $a_i |\rho_i, \theta_i\rangle = \sqrt{\rho_i} e^{i\theta_i} |\rho_i, \theta_i\rangle$,

$$\begin{aligned} & \langle \text{SF} | e^{iH_{\text{DW}}t} a_i^\dagger a_j e^{-iH_{\text{DW}}t} | \text{SF} \rangle \\ & \propto e^{i(\theta_j - \theta_i)} \exp \left\{ [(\rho_i + \rho_j)(\cos(Ut) - 1)] \right\} \\ & \times \exp \left\{ [2\sqrt{\rho_i \rho_j}(\cos(Vt) - 1)] \right\}, \end{aligned} \quad (8)$$

where $H_{\text{DW}} = \frac{U}{2}(n_i(n_i - 1) + n_j(n_j - 1)) + Vn_i n_j$. In the DW, the on-site U -term in Eq.(8) dominates over the NN V -term, and the oscillation period approximately is given by $2\pi/U$. This explains the result in Fig. 11.

In order to verify the above expectation, we study the cases of various τ_Q 's, and show F_o and vortex configurations for $J/U \approx 0$ in Fig. 12. For $\tau_Q = 50$ and 200 , rather clear domain walls exist, and interestingly enough, large amount of vortices reside on these domain walls. Therefore, the SF phase coherence is destroyed. On the other hand for $\tau_Q = 300$, existence of domain walls are not so

clear, and the number of vortices is small and vortices seem locate rather randomly. We expect that this is the origin for the oscillating behavior of F_o . In summary, we observe that for slower quench from the SF to DW, the SF amplitude $|\Psi|$ is getting smaller but the SF phase coherence is getting stronger compared to the faster quench as the vortex distribution and the first-order correlation F_o indicate.

V. CONCLUSION AND DISCUSSION

In this paper, we studied the EBHM on the square lattice, which is expected to be realized by the ultra-cold atomic gases and quantum simulated. We first clarify the phase diagram of the system near the unit filling and $V/U = 0.375$. There are three phases, the WD, SS and SF. Then we studied the non-equilibrium quench dynamics by varying the hopping amplitude as a function of time.

In the quench dynamics from the DW to SS, we observed the time evolution of the SF amplitude and verified that it exhibits similar behavior in the Mott to SF second-order phase transition. The correlation length of the SF order, vortex density, t and t_{eq} , all exhibit the scaling laws with respect to the quench time τ_Q . By using the KZ scaling hypothesis, the values of critical exponents ν and z are estimated from our numerical simulations, and we found that they are fairly close to those of the 3D XY model.

Next, we investigated the quench dynamics from the DW to SF through the SS. We verified that the phase degrees of freedom of the SF order parameter experiences the coarsening process as in the Mott to SF transition. The correlation length of the SF was also measured and we found that it gets large in the SF regime. This result implies that a SF at finite temperature forms as a result of the energy injection by the quench. On the other hand, the DW order smoothly decreases after passing the static transition point to the SS and vanishes at the transition to the SF.

Finally, we investigated the quench dynamics from the SF to DW. The SF amplitude starts to decrease at the SF-SS transition point J_{c2} . After passing the SS-DW transition point, it exhibits the oscillating behavior for $\tau_Q = 300$. Observation of the first-order correlation of the SF indicates that it is nothing but the collapse-revival phenomenon of the quenched SF correlation in the DW regime. Similar phenomenon was discussed for the SF-Mott quench dynamics in the previous paper.

We hope that phenomena that were investigated in this work will be observed in ultra-cold atomic experiments in the near future.

Recently, there appeared very interesting theoretical study on universality in the dynamics of quench phase transition [36]. There, by using equations of motion or Ginzburg-Landau-type arguments, the KZ scaling was re-derived. It is quite interesting to see how this approach

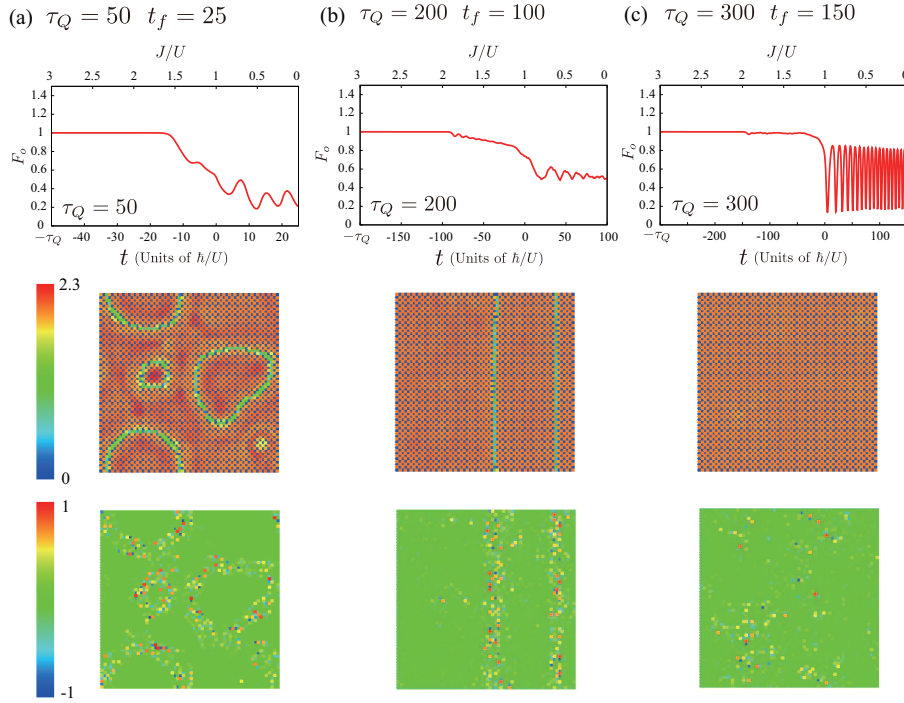


FIG. 12. Upper panel: First-order correlation function as a function of time for $\tau_Q = 50$, 200 and 300, Middle panel: Density profiles corresponding to the above times (Fig. 10), Lower panel: Vortex distributions corresponding to the above times.

is applied to the present multi-second-order phase transitions. This problem is under study, and results will be reported in a future publication.

ACKNOWLEDGMENTS

Y. K. acknowledges the support of a Grant-in-Aid for JSPS Fellows (No.17J00486).

[1] I. M. Georgescu, S. Ashhab, and F. Nori, Rev. Mod. Phys. **86**, 153 (2014).
[2] J. I. Cirac and P. Zoller, Nat. Phys. **8**, 264 (2012).
[3] I. Bloch, J. Dalibard, and W. Zwerger, Rev. Mod. Phys. **80**, 885 (2008).
[4] M. Lewenstein, A. Sanpera, and V. Ahufinger, *Ultracold Atoms in Optical Lattices: Simulating Quantum Many-body Systems* (Oxford University Press, Oxford, 2012).
[5] T. W. B. Kibble, J. Phys. A: Math. Gen. **9**, 1387 (1976).
[6] T. W. B. Kibble, Phys. Rep. **67**, 183 (1980).
[7] W. H. Zurek, Nature **317**, 505 (1985).
[8] W. H. Zurek, Acta Phys. Pol. B **24**, 1301 (1993).
[9] W. H. Zurek, Phys. Rep. **276**, 177 (1996).
[10] See for example, A. del Campo and W. H. Zurek, Int. J. Mod. Phys. A **29**, 1430018 (2014).
[11] N. Navon, A. L. Gaunt, R. P. Smith, and Z. Hadzibabic, Science **347**, 167 (2015).
[12] J. Beugnon and N. Navon, J. Phys. B: At. Mol. Opt. Phys. **50**, 022002 (2017).
[13] L. Chomaz, L. Corman, T. Bienaime, R. Desbuquois, C. Weitenberg, S. Nascimbene, J. Beugnon, and J. Dalibard, Nature Comm. **6**, 6172 (2015).
[14] J. Dziarmaga, Phys. Rev. Lett. **95**, 245701 (2005).
[15] A. Polkovnikov, Phys. Rev. B **72**, 161201(R) (2005).
[16] W. H. Zurek, U. Dorner, and P. Zoller, Phys. Rev. Lett. **95**, 105701 (2005).
[17] A. Chandran, A. Erez, S. S. Gubser, and S. L. Sondhi, Phys. Rev. B **86**, 064304 (2012).
[18] J. Sonner, A. del Campo, and W. H. Zurek, Nature Communication **6**, 7406 (2015).
[19] A. Francuz, J. Dziarmaga, B. Gardas, and W. H. Zurek, Phys. Rev. B **93**, 075134 (2016).
[20] D. Chen, M. White, C. Borries, and B. DeMarco, Phys. Rev. Lett. **106**, 235304 (2011).

- [21] S. Braun, M. Friesdrof, S. S. Hodgman, M. Schreiber, J. P. Ronzheimer, A. Riera, M. del Rey, I. Bloch, J. Eisert, and U. Schneider, *Proc. Nat. Acad. Sci. USA* **112**, 3641 (2015).
- [22] M. Anquez, B. A. Robbins, H. M. Bharath, M. Boguslawski, T. M. Hoang, and M. S. Chapman, *Phys. Rev. Lett.* **116**, 155301 (2016).
- [23] L. W. Clark, L. Feng, and C. Chin, *Science* **354**, 606 (2016).
- [24] J-M. Cui, Y-F. Huang, Z-W. Wang, D-Y. Cao, J. Wang, W-M. Lv, L. Luo, A. del Campo, Y-J. Han, C-F. Li, and G-C. Guo, *Sci. Rep.* **6**, 33381 (2016).
- [25] K. Shimizu, Y. Kuno, T. Hiraho, and I. Ichinose, *Phys. Rev. A* **97**, 033626 (2018).
- [26] K. Shimizu, T. Hirano, J. Park, Y. Kuno, and I. Ichinose, arXiv:1803.02548.
- [27] T. Kimura, *Phys. Rev. A* **84**, 063630 (2011).
- [28] T. Ohgoe, T. Suzuki, and N. Kawashima, *Phys. Rev. B* **86**, 054520 (2012).
- [29] M. Iskin, *Phys. Rev. A* **83**, 051606 (R) (2011).
- [30] J. Dziarmaga, *Adv. Phys.* **59**, 1063 (2010).
- [31] U. R. Fischer and B. Xiong, *Phys. Rev. A* **84**, 063635 (2011).
- [32] S. Will, T. Best, U. Schneider, L. Hackermu, and I. Bloch, *Nature* **465**, 197 (2010).
- [33] M. Buchhold, U. Bissbort, S. Will, and W. Hofstetter, *Phys. Rev. A* **84**, 023631 (2011).
- [34] C. Kollath, A. M. Lauchli, and E. Altman, *Phys. Rev. Lett.* **98**, 180601 (2007).
- [35] F. Meinert, M. J. Mark, E. Kirilov, K. Lauber, and P. Weinmann, *Phys. Rev. Lett.* **112**, 193003 (2014).
- [36] G. Nikoghosyan, R. Nigmatullin, and M. B. Plenio, *Phys. Rev. Lett.* **116**, 080601 (2016).